EARTHQUAKE ENGINEERING AND STRUCTURAL DYNAMICS, VOL. 3, 157–169 (1974)

SCATTERING OF PLANE SH WAVES BY A SEMI-ELLIPTICAL CANYON

H. L. WONG* AND M. D. TRIFUNAC†

California Institute of Technology, Pasadena, California, U.S.A.

SUMMARY

In this paper we analyse the two-dimensional scattering and diffraction of plane SH waves by a semi-elliptical canyon. The exact series solution of the problem, for general angle of incidence of the plane SH waves, has been used to examine the dependence of surface amplifications inside and near the canyon. The nature of ground motion has been found to depend on two key parameters:

(a) The angle of incidence.

(b) The ratio of the canyon width to the wave length of incident SH waves.

For short incident waves surface displacement amplitudes change rapidly from one point to another, while for the long waves and shallow canyons displacement amplitudes display only minor departure from the uniform half-space amplification of 2. For shallow canyons and long incident waves, the angle of incidence introduces only minor changes into the overall behaviour of surface amplitudes. For deep canyons and nearly grazing incidences, a prominent shadow zone is realized behind the canyon.

INTRODUCTION

The purpose of this paper is to add the exact solution of the problem of scattering and diffraction of plane SH waves by a semi-elliptical canyon to the limited collection of exact or approximate solutions with the effects of surface topography on elastic wave propagation.[1–7] Though limited by its two-dimensional nature and simple plane SH wave excitation, this problem is better suited for approximate evaluation of the amplification effects near topographic features that can be approximated by an ellipse than the solution one of us recently presented for the canyon of semi-circular cross-section.[7]

The effects of surface topography on amplification and attenuation of strong earthquake ground motion will no doubt receive more attention in earthquake engineering research when sophisticated finite element and finite difference codes become available for use on a routine basis. However, for the development of such codes and other approximate solutions, it is essential to have available various exact solutions so that the approximate methods can be critically tested and evaluated. The solution obtained in this paper can also be used to evaluate the shielding effects of a trench.

THE MODEL

The two-dimensional model to be analysed is shown in Figure 1. It consists of an elastic homogeneous half-space ($y<0$ for a shallow canyon or $x>0$ for a deep canyon) from which one half of a cylinder of elliptical cross-section has been removed. The half-width of the canyon, A, will be used to normalize the dimensionless frequencies. Another parameter of length, a, the half-focal length of the ellipse, will be used to vary the depth of the cavity.

---

* Graduate Student in Applied Mechanics.

† Assistant Professor of Applied Science.

Received 4 March 1974

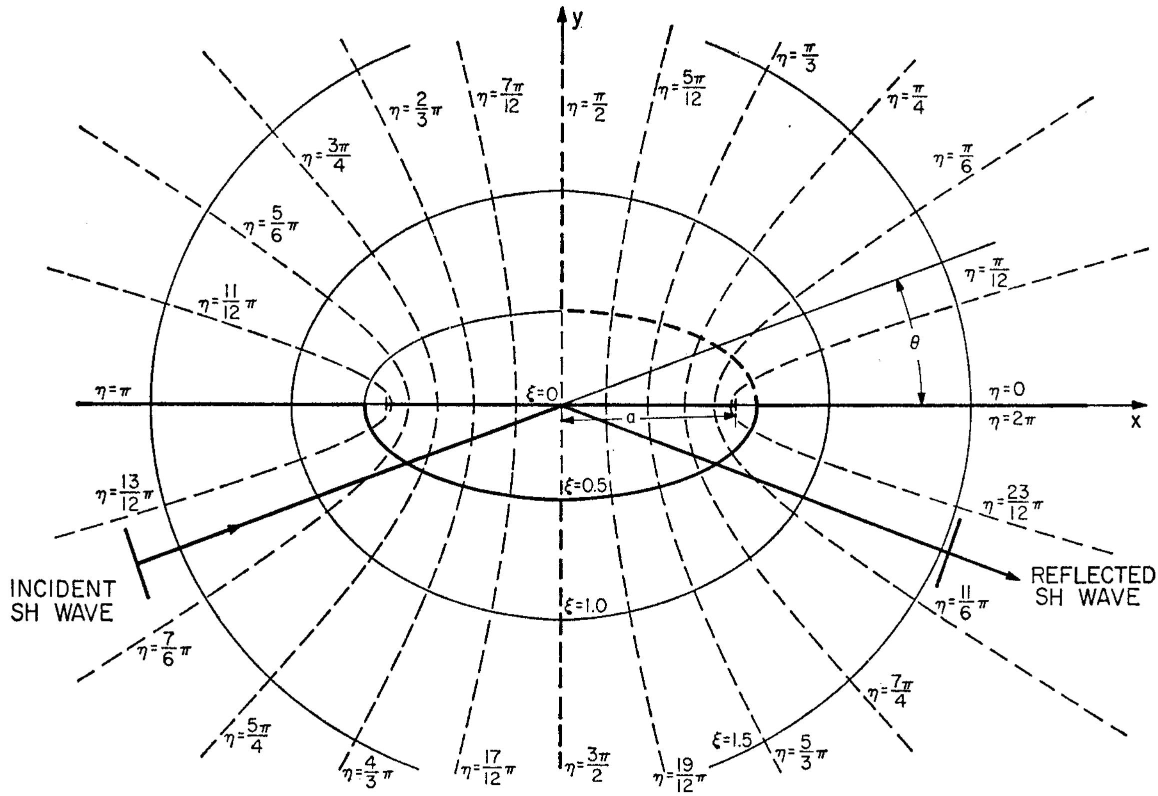

Figure 1. Semi-elliptical canyon, the surrounding half-space and the co-ordinate system

The cartesian co-ordinate system $x-y$ is transformed into the elliptical co-ordinates $\xi-\eta$ for convenience. The co-ordinate transformation relating rectangular and elliptical co-ordinates is

$$\left.\begin{aligned} x &= a\cosh\xi\cos\eta \\ y &= a\sinh\xi\sin\eta \end{aligned}\right\} \quad \begin{aligned} &0\leqslant\xi<\infty \\ &0\leqslant\eta\leqslant 2\pi \end{aligned}$$

where ξ is the 'radial co-ordinate' and η is the 'angular co-ordinate'.

Excitation

We shall assume that the excitation of the half space u_z^i consists of an infinite train of plane SH waves with frequency ω, with non-zero motion in the z (out-of-plane) direction only and the angle of incidence θ (Figure 1)

$$u_z^i = \exp\left[-i\omega\left(t-\frac{x}{c_x}-\frac{y}{c_y}\right)\right]$$

where c_x and c_y are the phase velocities along the x and y co-ordinates ($c_x = \beta/\cos\theta, c_y = \beta/\sin\theta$).

Solution of the problem for shallow canyon

The two-dimensional Helmholtz equation in cartesian co-ordinates for a displacement field ψ

$$\frac{\partial^2\psi}{\partial x^2}+\frac{\partial^2\psi}{\partial y^2}+K^2\psi = 0$$

becomes

$$\frac{\partial^2\psi}{\partial\xi^2}+\frac{\partial^2\psi}{\partial\eta^2}+a^2K^2(\cosh^2\xi-\cos^2\eta)\psi = 0 \tag{1}$$

for the elliptical co-ordinates. The solution of (1) is readily obtained by the method of separation of variables with

$$\psi(\xi,\eta) = Z(\xi)\, H(\eta)$$

Equation (1) then separates into the two ordinary differential equations:

$$\frac{d^2 H}{d\eta^2} + (b - 2q\cos 2\eta)\, H = 0 \tag{2a}$$

and

$$\frac{d^2 Z}{d\xi^2} - (b - 2q\cosh 2\xi) Z = 0 \tag{2b}$$

where

$$q = \frac{1}{4} a^2 K^2 = \frac{1}{4}\frac{a^2\omega^2}{\beta^2}$$

b is the characteristic number of the equations, K is the wave number and β is the shear-wave velocity. The solutions of equation (2a) are Mathieu functions. They depend on both b and q and may be expanded into Fourier series as follows:

$$ce_{2m}(\eta, q) = \sum_{r=0}^{\infty} A_{2r}^{(2m)}(q) \cos 2r\eta$$

$$se_{2m+2}(\eta, q) = \sum_{r=0}^{\infty} B_{2r}^{(2m+2)}(q) \sin 2r\eta$$

$$ce_{2m+1}(\eta, q) = \sum_{r=0}^{\infty} A_{2r+1}^{(2m+1)}(q) \cos (2r+1)\eta$$

$$se_{2m+1}(\eta, q) = \sum_{r=0}^{\infty} B_{2r+1}^{(2m+1)}(q) \sin (2r+1)\eta$$

The solutions of equation (2b) are called radial Mathieu functions, and the ones of interest for this problem are $Mc_{2m}^{(1)}$, $Mc_{2m+1}^{(1)}$, $Mc_{2m}^{(3)}$ and $Mc_{2m+1}^{(3)}$. These reduce to the Bessel functions and Hankel functions of the first kind as q approaches 0. For numerical calculations, the radial functions may be expressed in series of Bessel functions.

$$\begin{cases} Mc_{2m}^{(1)} = \dfrac{1}{A_0^{(2m)}} \displaystyle\sum_{r=0}^{\infty} (-1)^{r+m} A_{2r}^{(2m)} J_r(\mu_1) J_r(\mu_2) \\[2ex] Mc_{2m+1}^{(1)} = \dfrac{1}{A_1^{(2m+1)}} \displaystyle\sum_{r=0}^{\infty} (-1)^{r+m} A_{2r+1}^{(2m+1)} [J_r(\mu_1) J_{r+1}(\mu_2) + J_r(\mu_2) J_{r+1}(\mu_1)] \end{cases}$$

$$\begin{cases} Mc_{2m}^{(3)} = \dfrac{1}{A_0^{(2m)}} \displaystyle\sum_{r=0}^{\infty} (-1)^{r+m} A_{2r}^{(2m)} J_r(\mu_1) H_r^{(1)}(\mu_2) \\[2ex] Mc_{2m+1}^{(3)} = \dfrac{1}{A_1^{(2m+1)}} \displaystyle\sum_{r=0}^{\infty} (-1)^{r+m} A_{2r+1}^{(2m+1)} [J_r(\mu_1) H_{r+1}^{(1)}(\mu_2) + J_{r+1}(\mu_1) H_r^{(1)}(\mu_2)] \end{cases}$$

where $\mu_1 = \sqrt{(q)}\exp(-\xi)$ and $\mu_2 = \sqrt{(q)}\exp(\xi)$. Further details on the theory of Mathieu functions are available in literature on special functions[8–10] and will not be presented here.

The representation of the plane wave $\exp(i\omega t)\, u_z^i = \exp[iK(x\cos\theta + y\sin\theta)]$ may be given by the series of Mathieu functions, dropping $\exp(i\omega t)$ dependence, as

$$u_z^i = 2\sum_{m=0}^{\infty} i^m\, ce_m(\eta,q)\, Mc_m^{(1)}(\xi,q)\, ce_m(\theta,q)$$

$$+2\sum_{m=1}^{\infty} i^m\, se_m(\eta,q)\, Ms_m^{(1)}(\xi,q)\, se_m(\theta,q)$$

where the angle θ is measured from the positive x-axis to the wave front normal. The half-space problem can then be solved by superposing another plane wave, u_z^r, travelling with an angle $-\theta$ and the wave motion in the absence of the canyon becomes

$$u_z^i + u_z^r = 4\sum_{m=0}^{\infty} i^m\, ce_m(\eta,q)\, Mc_m^{(1)}(\xi,q)\, ce_m(\theta,q) \tag{3}$$

The wave reflected from the elliptic canyon must satisfy equations (2) and the following boundary conditions:

$$\text{(i)}\quad \frac{\mathrm{d}H(\eta)}{\mathrm{d}\eta} = 0 \quad \text{at } \eta = 0, -\pi \tag{4a}$$

$$\text{(ii)}\quad \frac{\mathrm{d}Z(\xi)}{\mathrm{d}\xi} = 0 \quad \text{at } \xi = \xi_0 \tag{4b}$$

Satisfying equations (2) and (4a), we have the outgoing wave solution for the wave reflected from the elliptical canyon as

$$u_z^R = \sum_{m=0}^{\infty} [a_{2m}\, Mc_{2m}^{(3)}(\xi,q)\, ce_{2m}(\eta,q) + b_{2m+1}\, Mc_{2m+1}^{(3)}(\xi,q)\, ce_{2m+1}(\eta,q)] \tag{5}$$

The total solution u, which is the sum of equations (3) and (5), must satisfy the boundary condition (4b). The coefficients a_{2m} and b_{2m+1} then become

$$\left.\begin{aligned} a_{2m} &= 4(-1)^{m+1}\frac{ce_{2m}(\theta,q)\, Mc_{2m}^{(1)\prime}(\xi_0,q)}{Mc_{2m}^{(3)\prime}(\xi_0,q)} \\ b_{2m+1} &= 4i(-1)^{m+1}\frac{ce_{2m+1}(\theta,q)\, Mc_{2m+1}^{(1)\prime}(\xi_0,q)}{Mc_{2m+1}^{(1)\prime}(\xi_0,q)} \end{aligned}\right\} \tag{6}$$

where ',' on the radial Mathieu functions designates differentiation with respect to ξ. The exact solution is therefore

$$u = 4\left\{\sum_{m=0}^{\infty}(-1)^m\, ce_{2m}(\eta,q)\, ce_{2m}(\theta,q)\left[Mc_{2m}^{(1)}(\xi,q) - \frac{Mc_{2m}^{(1)\prime}(\xi_0,q)}{Mc_{2m}^{(3)\prime}(\xi_0,q)}Mc_{2m}^{(3)}(\xi,q)\right]\right\}$$

$$+4i\left\{\sum_{m=0}^{\infty}(-1)^m\, ce_{2m+1}(\eta,q)\, ce_{2m+1}(\theta,q)\left[Mc_{2m+1}^{(1)}(\xi,q) - \frac{Mc_{2m+1}^{(1)\prime}(\xi_0,q)}{Mc_{2m+1}^{(3)\prime}(\xi_0,q)}Mc_{2m+1}^{(3)}(\xi,q)\right]\right\}. \tag{7}$$

Solution of the problem for a deep canyon

In the case we have just considered, the major axis of the ellipse lies on the x-axis, and the deepest canyon to which the above solution applies is limited to that of a semi-circle. For a solution of a deeper canyon, the major axis must be rotated by $\pi/2$, counter clockwise, so that the half-space is defined by $x > 0$.

With

$$\exp[iK(x\cos\theta+y\sin\theta)] = 2\sum_{m=0}^{\infty} i^m ce_m(\eta,q)\, Mc_m^{(1)}(\xi,q)\, ce_m(\theta,q)$$

$$+2\sum_{m=0}^{\infty} i^m se_m(\eta,q)\, Ms_m^{(1)}(\xi,q)\, se_m(\theta,q)$$

the incident wave is now defined by the angle $\pi-\theta$ relative to the x-axis, while the angle of the reflected wave is θ. The sum of incident and reflected waves gives the solution for the infinite half-space Since $\cos(m\pi-m\theta) = (-1)^m \cos m\theta$ and $\sin(m\pi-m\theta) = (-1)^{m+1}\sin m\theta$, this solution is

$$u_z^i+u_z^r = 4\sum_{m=0}^{\infty} (-1)^m ce_{2m}(\eta,q)\, Mc_{2m}^{(1)}(\xi,q)\, ce_{2m}(\theta,q)$$

$$+4\sum_{m=0}^{\infty} i(-1)^m se_{2m+1}(\eta,q)\, Ms_{2m+1}^{(1)}(\xi,q)\, se_{2m+1}(\theta,q). \tag{8}$$

The boundary conditions now become

$$\text{(i)} \quad \frac{\mathrm{d}H(\eta)}{\mathrm{d}\eta} \quad \text{at } \eta = \frac{\pi}{2}, -\frac{\pi}{2} \tag{9a}$$

$$\text{(ii)} \quad \frac{\mathrm{d}Z(\xi)}{\mathrm{d}\xi} \quad \text{at } \xi = \xi_0 \tag{9b}$$

satisfying the wave equation (2) and boundary condition (9a), we have the outgoing wave solution for the wave reflected from the elliptical valley as

$$u_z^R = \sum_{m=0}^{\infty} c_{2m}\, Mc_{2m}^{(3)}(\xi,q)\, ce_{2m}(\eta,q) + \sum_{m=0}^{\infty} \mathrm{d}_{2m+1}\, Ms_{2m+1}^{(3)}(\xi,q)\, se_{2m+1}(\eta,q) \tag{10}$$

Substitution of equations (8) and (10) into the boundary condition (9b) yields

$$\left.\begin{aligned} c_{2m} &= 4(-1)^{m+1}\frac{ce_{2m}(\theta,q)\, Mc_{2m}^{(1)\prime}(\xi_0,q)}{Mc_{2m}^{(3)\prime}(\xi_0,q)} \\ \mathrm{d}_{2m+1} &= 4i(-1)^{m+1}\frac{se_{2m+1}(\theta,q)\, Ms_{2m+1}^{(1)\prime}(\xi_0,q)}{Ms_{2m+1}^{(3)\prime}(\xi_0,q)} \end{aligned}\right\} \tag{11}$$

The exact solution for the deep canyon is then

$$u = 4\left\{\sum_{m=0}^{\infty}(-1)^m ce_{2m}(\eta,q)\, ce_{2m}(\theta,q)\left[Mc_{2m}^{(1)}(\xi,q) - \frac{Mc_{2m}^{(1)\prime}(\xi_0,q)}{Mc_{2m}^{(3)\prime}(\xi_0,q)} Mc_{2m}^{(3)}(\xi,q)\right]\right\}$$

$$+4i\left\{\sum_{m=0}^{\infty}(-1)^m se_{2m+1}(\eta,q)\, se_{2m+1}(\theta,q)\left[Ms_{2m+1}^{(1)}(\xi,q) - \frac{Ms_{2m+1}^{(1)\prime}(\xi_0,q)}{Ms_{2m+1}^{(3)\prime}(\xi_0,q)} Ms_{2m+1}^{(3)}(\xi,q)\right]\right\} \tag{12}$$

SURFACE DISPLACEMENTS

From the earthquake engineering or seismological viewpoints the most important aspect of the foregoing analysis is the description of the surface displacement amplitudes in and around the elliptically shaped canyon. Regardless whether one has to find the possible amplification effects due to the local topography in evaluating the seismic safety of a nuclear power plant or to correct the spectra of a recorded seismogram, the answer to the problem will lie in the precise description of the amplitudes and phases of surface ground motions for incident waves with unit amplitudes, i.e. in the space-dependent transfer function.

For the excitation $u_z^i = \exp[-i\omega(t - x/c_x - y/c_y)]$ whose amplitude is 1 and whose phase changes linearly with x, the modulus of surface displacements in the uniform half-space is equal to 2. In the presence of a canyon the incident waves scatter and diffract around the canyon. The scattered and diffracted waves, u_z^R, interfere with the incident, u_z^i, and the reflected, u_z^r, motions and the resulting modulus of surface wave amplitudes may significantly depart from 2. To study these changes we characterize the motions by

$$\text{amplitude} \equiv [\mathrm{Re}^2(u) + \mathrm{Im}^2(u)]^{\frac{1}{2}} \tag{13}$$

and

$$\text{phase} \equiv \tan^{-1}[\mathrm{Im}(u)/\mathrm{Re}(u)] \tag{14}$$

where $u = u_z^i + u_z^r + u_z^R$. Both quantities depend on the shape of the elliptical canyon, frequency ω, velocity β and incident angle θ of incident SH waves and on the canyon width $2A$.

To simplify the description of the problem, we define the dimensionless parameter

$$\mathrm{ETA} = 2A/\lambda \tag{15}$$

which represents the dimensionless ratio of the canyon width to the wavelength of incident SH waves. Since

$$q = \tfrac{1}{4}a^2 K^2 \tag{16}$$

we have

$$\mathrm{ETA} = q^{\frac{1}{2}} \frac{2A}{\pi a} \tag{17}$$

Furthermore, because $\mathrm{ETA} = 2A/\beta T = A\omega/\pi\beta$, ETA can also be thought of as dimensionless frequency.

In the absence of the canyon the phase angle given by (14) would be the linear function of x,

$$\text{phase} = -\frac{\omega A}{\beta} \cos\theta \frac{x}{A} \tag{18}$$

For θ decreasing towards the grazing incidence ($\theta = 0$) and increasing $\omega A/\beta$, the negative slope of the phase with respect to the positive x/A axis would increase.

Figures 2 to 6 illustrate typical characteristics of amplitudes and phases of surface displacements for depth to width ratio of the canyon equal to 0·05, 0·15, 0·35, 0·71 and 1. These have been derived from the ratios of minor to major axes of an ellipse equal to 0·1, 0·3 and 0·7 for shallow cases in Figures 2, 3 and 4, and to 0·7 and 0·5 for deep canyon cases in Figures 5 and 6. Each figure presents amplitudes and phases for four values of dimensionless frequency ETA = 0·5, 1·0, 1·5 and 2·0. These we believe cover the most probable band of dimensionless frequencies that are likely to be encountered in earthquake engineering and strong-motion seismology applications. The phase diagrams have been shifted arbitrarily to have common zero phase for $x/A = 0$. This is in agreement with the convention used in the analysis of SH-wave scattering from a semi-circular canyon[7] and should prove convenient for relative comparison with the results in this paper.

In the mathematical formulation of the shallow canyon problem, the incidence angle θ has been measured as positive in the counter-clockwise direction from the positive x-axis to the positive normal of the plane incident wave (Figure 1). In the corresponding solution for the deep canyon, we found it convenient to rotate the co-ordinate system so as to keep the significant part of the mathematical formulation for the shallow case unchanged. To ease relative comparison of results in Figures 2 to 6 we decided, however, to present the two deep canyon cases in Figures 5 and 6 using the same co-ordinate system and the same convention for measuring θ as for Figures 2 to 4. Thus, for all figures $\theta = 0$ corresponds to the grazing incidence and $\theta = 90°$ to the vertical incidence.

Computation of the Mathieu functions represents a time-consuming and costly effort, since each function has to be evaluated by means of Bessel or sine and cosine series. Furthermore, the needed number of terms in the series representations (7) and (12) increases with increasing $|x|$ and q (i.e. increasing ETA). To cut this computational effort we used the constant number of terms for both series in (7) and (12) and approximately tested the accuracy of the finite sum by comparing the series with N and $N+1$ terms. For higher values of ETA we restricted the computation of amplitudes and phases to $x/A = 2{\cdot}5$ or $2{\cdot}0$ only. The resulting typical accuracy of all amplitudes and phases presented in Figures 2–6 is better than 1 per cent.

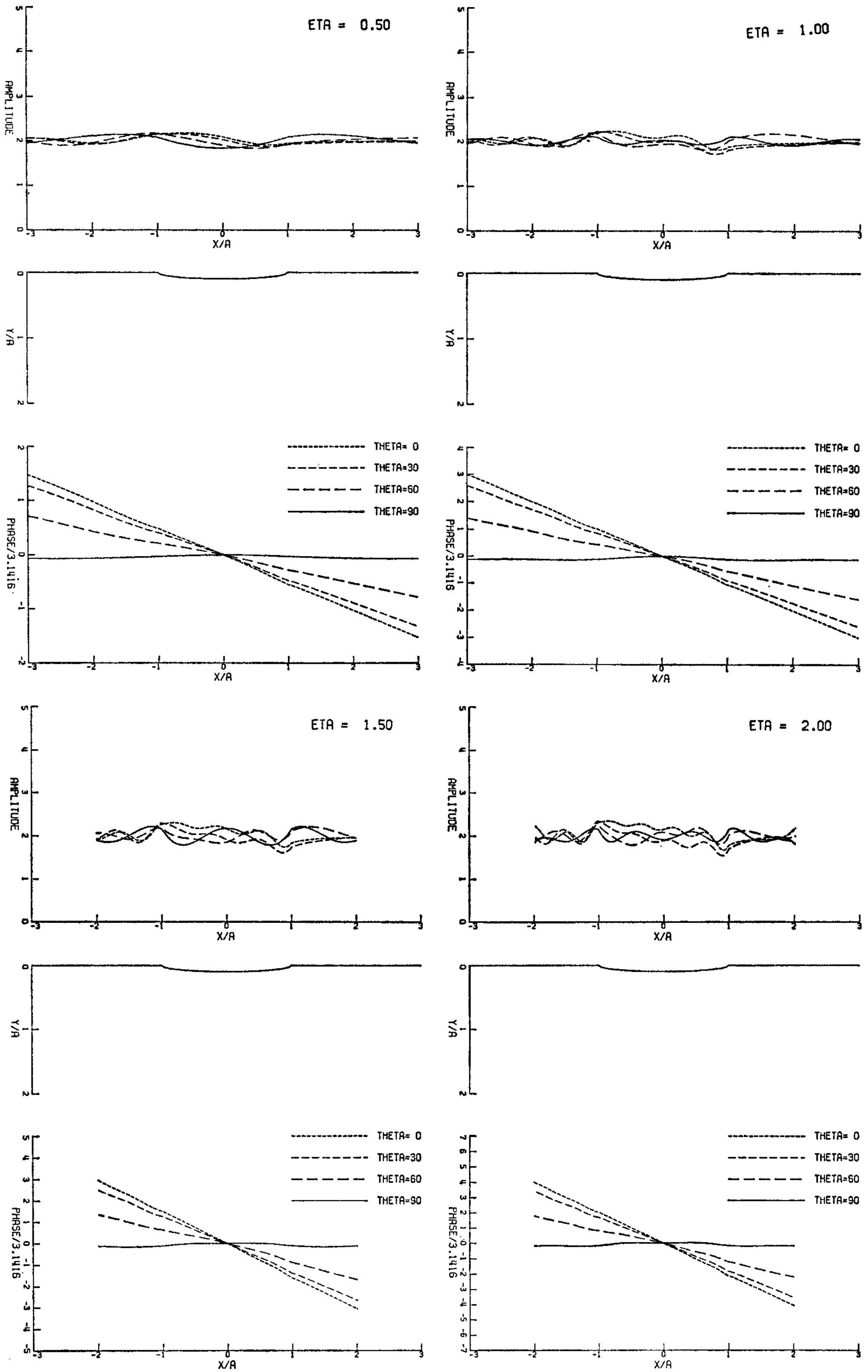

Figure 2. Surface displacement amplitudes and phases for incident SH waves. Canyon depth to width ratio is 0·05

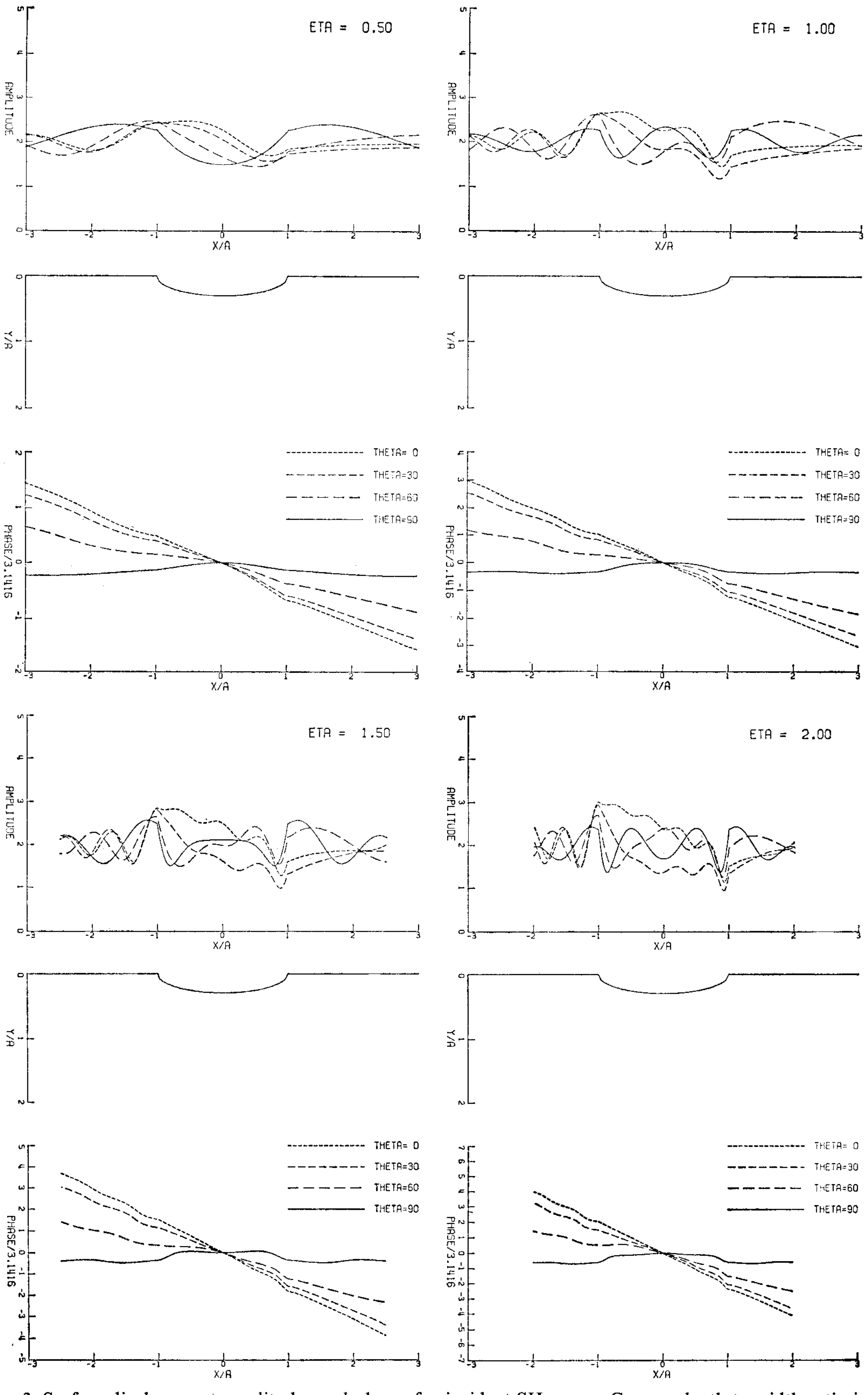

Figure 3. Surface displacement amplitudes and phases for incident SH waves. Canyon depth to width ratio is 0·15

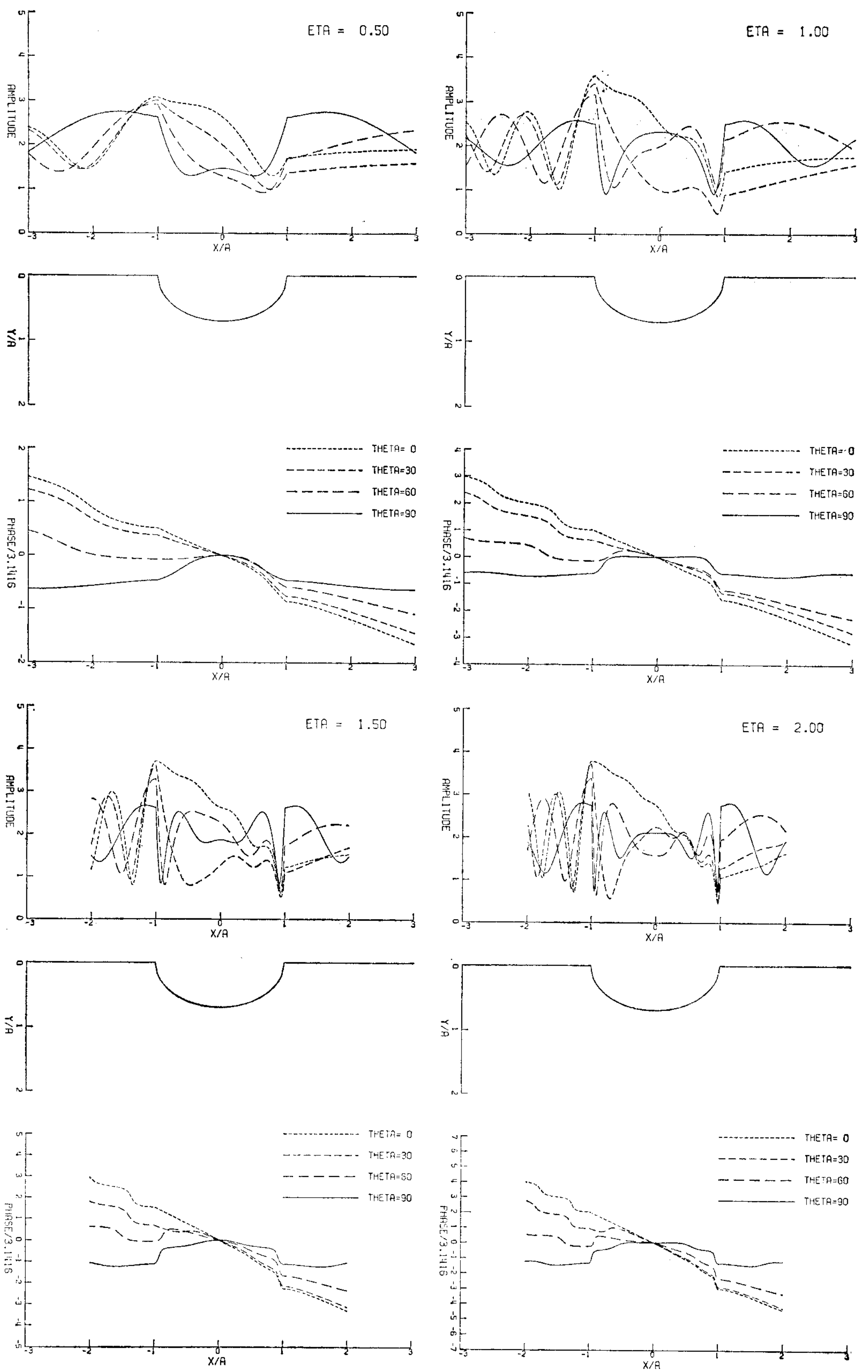

Figure 4. Surface displacement amplitudes and phases for incident SH waves. Canyon depth to width ratio is 0.35

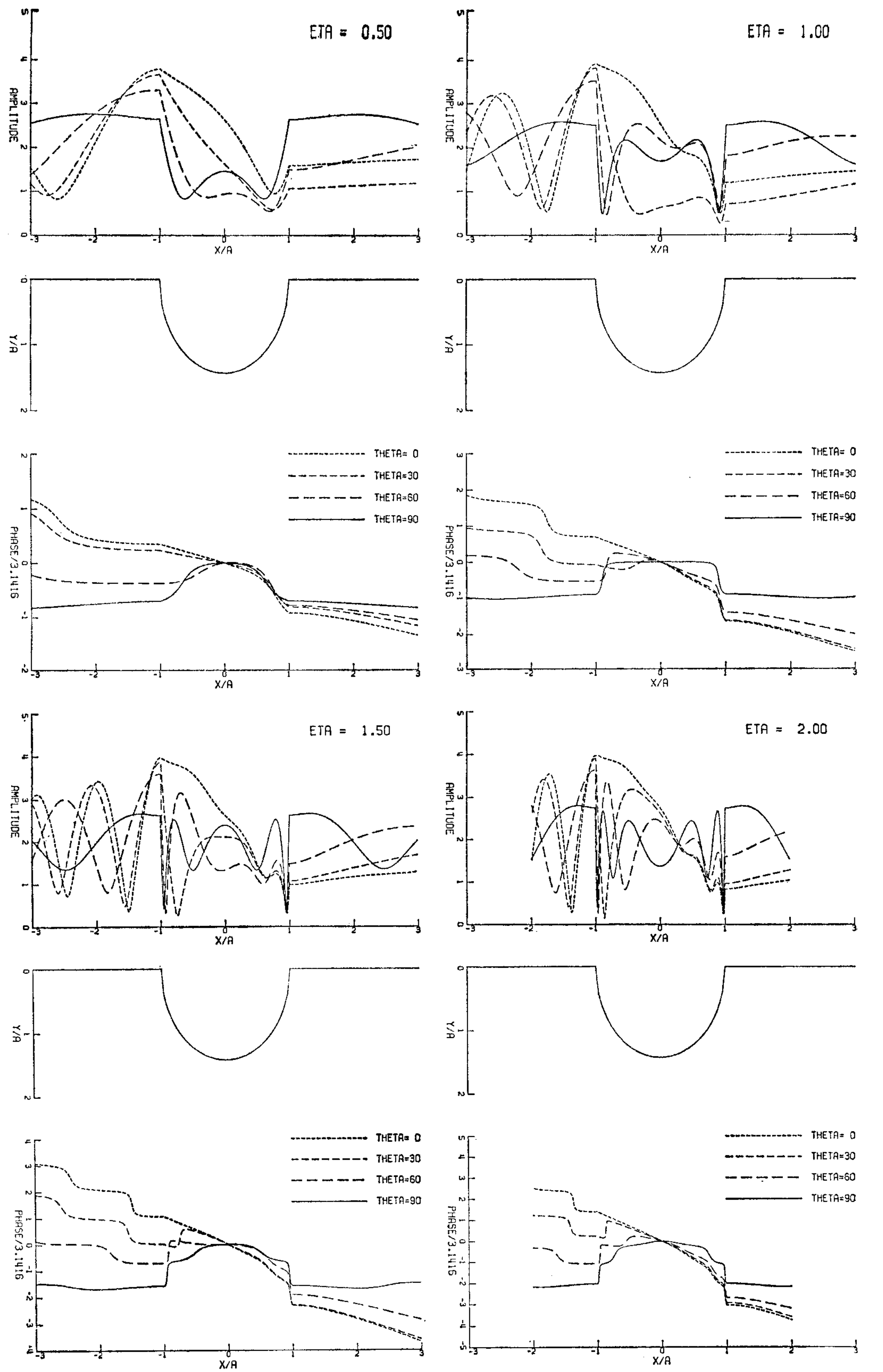

Figure 5. Surface displacement amplitudes and phases for incident SH waves. Canyon depth to width ratio is 0·71

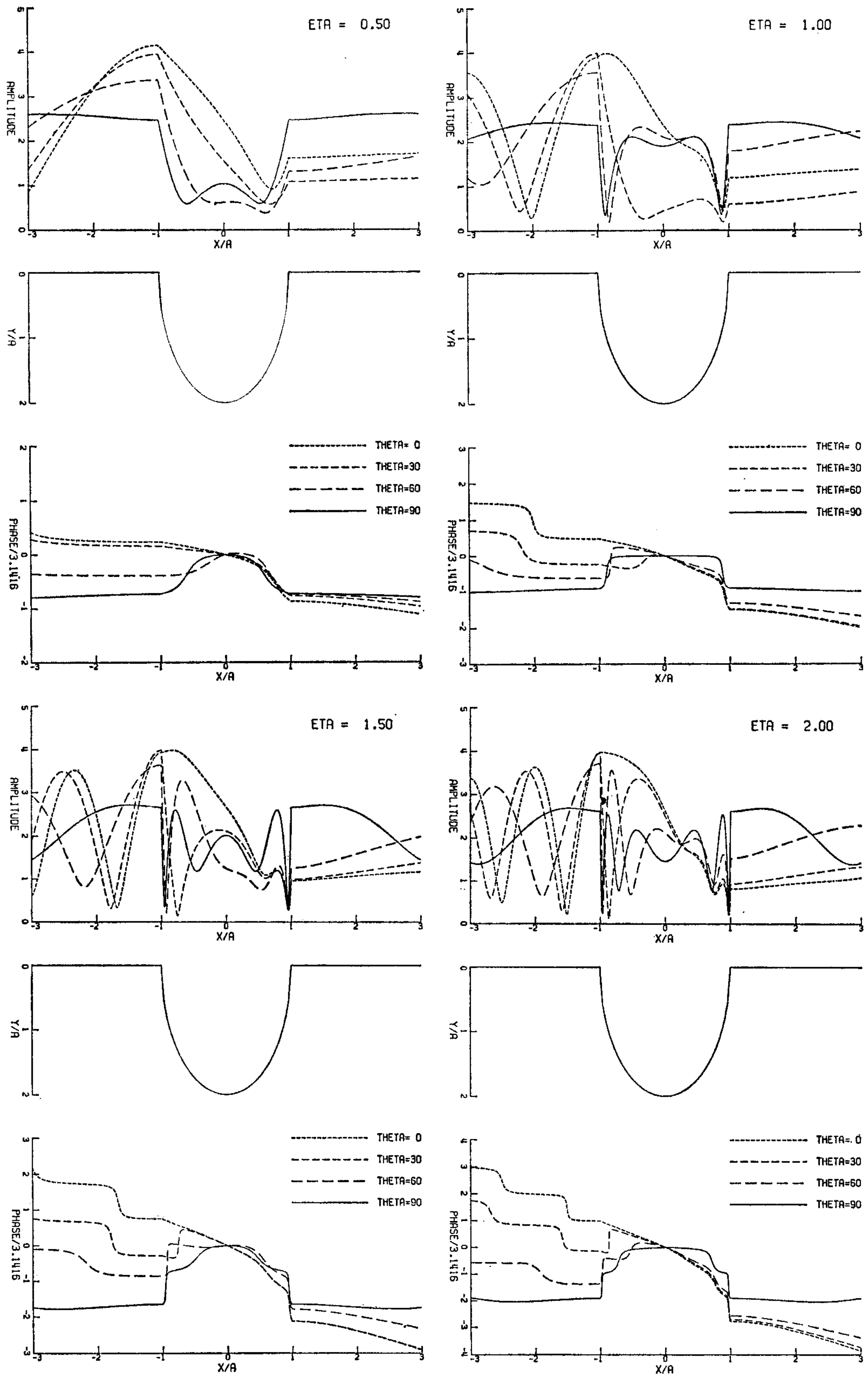

Figure 6. Surface displacement amplitudes and phases for incident SH waves. Canyon depth to width ratio is 1·0

Figure 2 shows the displacement amplitudes and phases for depth to width ratio of the canyon equal to 0·05. It is seen that the displacement amplitudes only slightly depart from the uniform half-space amplitudes equal to 2 and that the phases are quite close to the straight lines given by equation (18). All this points to the fact that this shallow canyon introduces only minor changes into the surface motions experienced by the uniform half-space. Even the shortest incident waves considered here (ETA = 2·0, Figure 2) do not feel the shallow canyon significantly, since their wavelength is ten times the canyon depth.

Figures 3 to 6 show progressively more complicated patterns of ground displacement amplitudes and phases. For deeper canyons a progressively stronger shadow zone is formed behind the canyon ($x/A > 1$). The standing wave pattern, resulting from the interference of incident and waves reflected from the canyon, is superimposed on the overall wave propagation to the right, and becomes more prominent as the height of the canyon wall at $x/A = -1$ becomes deeper. With increasing ETA and for deeper canyons we observe more prominent and more abrupt jumps of magnitude π in the phase diagrams. These jumps are most prominent at places where displacement amplitudes become very small or equal to zero. The physical meaning of these jumps is that the motion of the two points on the opposite side of the jump is 180° out of phase, i.e. that the points where a jump occurs experience predominantly torsional vibrations. The motion at these points is typically small or zero, since the displacement amplitudes go through their local minima there (Figures 3 to 6). In spite of the fact that different phase diagrams show varying degrees of abrupt or gradual jumps, they all have the same average trends which, in the limit when $|x/A| \to \infty$, tend to the linear phase relationship given by equation (18). This means that the overall wave motion remains the same as that for the half-space, i.e. from 'left' to 'right' in Figures 2 to 6. Since the canyon shape is symmetric, for vertical incidence of plane SH waves (THETA = 90), both displacement amplitudes and phases are symmetric.

The maximum possible amplitude of surface displacements is equal to 4 and for the incident wave propagation in the positive x direction it occurs at $x/A = -1$. It can be explained by the analogous quarter-space problem excited by plane SH waves and the twofold amplification analogous to the half-space amplification equal to 2.[7]

Since this paper presents merely a generalization of the SH-wave propagation near and around the canyon with semi-circular cross-section[7], we shall not repeat here the discussion dealing with the typical spectra and with the possible applications of the above results. Rather, we refer the reader to our previous paper[7] for these and other related considerations.

CONCLUSIONS

Some of the principal results that emerge from the foregoing analysis may be summarized as follows:

1. The amplification of surface displacements is always less than or equal to 2 (surface displacement amplitude is less than or equal to 4), since the most acute angle in the canyon cross-section is equal to 90°.[7]
2. The amplitudes and the patterns of surface displacements depend significantly on the direction of incident SH waves. For acute and grazing angles of incidence, a strong shadow zone may be developed behind the canyon. For the same excitation nearby standing wave motion may be set up in front of the canyon. This standing wave motion results from the interference of incident and waves reflected from the canyon wall.
3. The principal role of the canyon depth is that it determines the extent to which the above-mentioned amplification, standing wave pattern and the shadow zone are developed. For deeper canyons these effects increase.
4. A deep canyon or a trench could be used to shield against the incident waves with shallow or grazing angles of incidence. To obtain a reduction of about 50 per cent the depth of canyon would have to be of the order of the incident wave length.

ACKNOWLEDGEMENTS

We thank P. C. Jennings and J. E. Luco for the critical reading of this manuscript and some valuable remarks.

This work was supported by the National Science Foundation grants and the Earthquake Research Affiliates Program of the California Institute of Technology.

REFERENCES

1. C. B. Brown, 'Seismic energy transmission to deep-founded structures', *Bull Seism. Soc. Am.* **61**, 781–787 (1971).
2. D. Boore, 'The effect of simple topography on seismic waves: implications for the recorded accelerations at Pacoima Dam' (Abstract), Nat. Conf. Earthquake Eng., Los Angeles, California, 1972.
3. A. K. Mal and L. Knopoff, 'Transmission of Rayleigh waves past a step change in elevation', *Bull. Seism. Soc. Am.* **55**, 319–334 (1965).
4. W. C. Meecham, 'Variational method for the calculation of the distribution of energy reflected from a periodic surface, I', *J. Appl. Phys.* **27**, 361–367 (1956).
5. I. Abubakar, 'Reflection and refraction of plane SH waves at irregular interfaces, I, II', *J. Phys. of the Earth*, **10**, 1–14 and 15–20 (1962).
6. R. Sato, 'Diffraction of SH-waves at an obtuse-angled corner', *J. Phys. of the Earth*, **11**, 1–17 (1963).
7. M. D. Trifunac, 'Scattering of plane SH waves by a semi-cylindrical canyon', *Int. J. Earthq. Engng Struct. Dyn.* **1**, 267–281 (1973).
8. C. C. Mow and Y. H. Pao, 'The diffraction of elastic waves and dynamic stress concentrations', *RAND* Report, R-482-PR (1971).
9. P. M. Morse and H. Feshbach, *Methods of Theoretical Physics*, McGraw-Hill, New York (1953).
10. M. A. Abramowitz and I. A. Stegun, *Handbook of Mathematical Functions*, Ch. 20, Dover 0–486–61272–4, New York (1970).